PERGAMON

International Journal of Heat and Mass Transfer 41 (1998) 3255–3264

International Journal of HEAT and MASS TRANSFER

Heat transfer analysis of buoyancy-assisted mixed convection with asymmetric heating conditions

Xiaodong Zhang, Sandip Dutta*

Department of Mechanical Engineering, University of South Carolina, Columbia, SC 29208, U.S.A.

Received 8 July 1997; in final form 27 December 1997

Abstract

Experimental measurements and analysis of buoyancy-assisted mixed convection in a vertical square channel with asymmetric heating conditions are presented. Two opposite sides of the test section are heated in four designed heating models and the other two sides of the square channel are insulated. The Reynolds number is varied from 200 to 11 200 and the buoyancy parameter, Gr/Re^2, is varied from 0.02 to 200. The local heat transfer coefficient increases with increasing buoyancy parameter. Specifically, the Nusselt number ratio, Nu/Nu_0, is observed to be enhanced significantly with the increased turbulent mixing caused by more irregular heating conditions.

Nomenclature

$A_{channel}$ cross-section area of the square channel
A_{plate} area of the copper plate on which heaters and thermocouples are mounted
Bo buoyancy number [1]: $Bo = 8\cdot 10^4\cdot\rho^2\cdot g\cdot\beta\cdot q''\cdot D^4/k\mu^2/(Re^{3.425}\cdot Pr^{0.8})$
D, L hydraulic diameter and length of the heated channel
g gravitational acceleration constant
Gr Grashof number: $Gr = \rho^2\cdot g\cdot\beta\cdot(T_w - T_{in})\cdot D^3/\mu^2$
h, k convective heat transfer coefficient and thermal conductivity of water
Nu local Nusselt number: $Nu = hD/k$
Nu_0 Nu of fully developed turbulent pipe flow, from Incropera and Dewitt [2]:

$$Nu_0 = 1.86\cdot\left(Re\cdot Pr\cdot\frac{D}{L}\right)^{1/3} \text{ for } Re \leqslant 3000,$$

otherwise

$$Nu_0 = \left(\frac{f}{8}\cdot(Re-1000)\cdot Pr\right)\Bigg/\left(1+12.7\cdot\left(\frac{f}{8}\right)^{1/2}\cdot(Pr^{2/3}-1)\right)$$

where $f = (0.79\cdot\ln Re - 1.64)^{-2}$
$\overline{Nu}$ average Nusselt number
Pr laminar Prandtl number of water
q''_{total}, q''_{loss} total heat flux applied and heat flux lost to surroundings in each copper plate
Re Reynolds number: $Re = \rho\cdot V\cdot D/\mu$
T_w, T_{in}, T_b local wall temperature, inlet, and bulk water temperatures
V average axial velocity through the channel.

Greek symbols
β volume expansion coefficient of water
μ laminar viscosity of water
ρ density of water.

1. Introduction

Mixed convection is defined as heat transfer situations where both natural convection and forced convection heat transfer mechanisms interact. In a vertical passage, the internal main flow can be either upward or downward. The upward forced flow is termed 'assisted' flow

* Corresponding author. Tel.: 001 803 777 8013; fax.: 001 803 777 0106; e-mail: dutta@engr.sc.edu.

0017-9310/98 $19.00
PII: S0017-9310(98)00027-1

because the natural convection created by buoyancy is in the same direction as the bulk flow. In contrast, the downward flow is called 'opposed' flow based on its direction opposite to the natural convection.

In the past twenty years, mixed convection in a vertical heated channel has received considerable attention due to its extensive practical applications, including turbine rotor blade internal cooling systems, cooling of nuclear reactors, and electronic components. Many studies, both theoretical and experimental, exist in the literature on mixed convection. In the 1970s, Buhr [3] reported the distortion of velocity and turbulence distribution profile under the influence of buoyancy. Measurements in a turbulent flow of mercury revealed that the velocity as well as the nature of turbulence was affected by the presence of a heat flux. Nusselt numbers were significantly dependent on the Peclet number. The laminar and turbulent free convection with a non-Newtonian fluid were studied by Emery *et al.* [4] and a layered up and down flow structure was observed in a heated enclosure. Maitra and Raju [5] investigated mixed convection in a vertical annulus both theoretically and experimentally. However, their theoretical predictions gave much lower results than the measured Nusselt numbers. Mixed convection in inclined rectangular ducts was investigated by Ou et al. [6] and their numerical prediction showed noticeable secondary flow development in inclined channels, thus increasing flow mixing. A significant increase in the Nusselt number was observed with increasing the Rayleigh number. Abdelmeguid and Spalding [7] showed that a remarkable distortion occurs in the flow distribution in heated ducts.

A modified version of the k–ε turbulence model was applied to two limiting cases of turbulence buoyant wall jets by Ljuboja and Rodi [8]. Their model predicted those limiting cases with accuracy sufficient for practical purposes under the main assumption that turbulence is nearly in local equilibrium. Ramachandran et al. [9] reported their measurements and predictions for Laminar mixed convection airflow. The local Nusselt number was found increasing for assisted flow and decreasing for opposed flow with increasing buoyancy parameters. Their experimental measurements and numerical predictions agreed well with each other. Krishnamurthy and Gebhart [10] presented their studies on transition of mixed convection flow in a vertical channel. A power averaging of natural and forced convection was showed to represent the mixed convection heat transfer coefficients. Heat transfer coefficients in mixed convection were higher than the natural or the forced convection results depending on the flow and heating conditions. Shai and Barnea [11] reported their observations of mixed convection with a uniform heat flux. Two regions were found in the opposed mixed convection, one was dominated by forced convection and the other one by natural convection. A buoyancy parameter, Gr/Re^2, dominated 2-D mixed convection on a flat plate [12]. Tewari and Jaluria [13] analyzed mixed convection with discrete thermal sources on horizontal and vertical surfaces. They observed that the upstream heat source could affect the heat transfer performance of the downstream heat source if the separation distance is less than three strip widths. The magnitude of the effect was dependent on the orientation of the heat sources.

Lin and Hsieh [14] measured the effects of ribs in buoyancy driven flow. According to Cheng et al. [15] flow reversal adjacent to the cooler wall was dependent on the Re/Gr ratio in a mixed convection. Gau et al. [16] studied the flow structure and heat transfer at relatively large buoyancy parameter, Gr/Re^2, in a heated vertical channel. A V-shaped recirculation rendered the flow highly unstable and led to generation of eddies and vortices in the downstream region. The increasing Reynolds number pushed the reversed flow downstream and made the recirculating region wider. Choi and Ortega [17] investigated the mixed convection in an inclined channel with a discrete heat source. Heat transfer of the source strongly depended on the inclination angle, γ, for $\gamma \geqslant 45°$. But the influence of γ was negligible for $0° \leqslant \gamma \leqslant 45°$. Cheng and Weng [18] found that the flow reversal is dependent on the critical parameter Gr/Re. Their investigation on buoyancy driven flow separation was extended by Cheng and Yang [19] in vertical channels with fin arrays. Their results showed that with sufficiently strong heating a series of buoyancy-induced recirculation bubbles would be rendered in vertical channels. Fu et al. [20] modified the Jackson correlation [21] for their design applications in mixed convection with airflow. Huang et al. [22] discussed the mixed convection flow and heat transfer in a heated vertical convergent channel. Flow reversal was reported for both assisting and opposing flow; and this buoyancy opposed flow reversal significantly enhanced the heat transfer along the heated wall.

Joye [23] compared his experimental results with the published correlations for opposed mixed convection in a vertical tube with Grashof number, Gr, variation. His data with Gr as a parameter showed reduced heat transfer enhancements with an increasing Grashof number. The previous published correlations predicted his experimental data moderately well except for near and in the asymptotic region. Ligrani et al. [24] performed their extensive research for mixed convection in straight and curved channels with buoyancy orthogonal to the forced flow. Gau et al. [25] extended their research to pure forced and mixed convection flow and heat transfer in a divergent vertical channel. The channel divergence destabilized the downstream flow and noticeably enhanced the heat transfer. Wang and Cheng [26] presented their analytical results for flow transition in a mixed convection rotating flow that showed complex secondary flows due to separation in buoyant flow. Velidandla et al. [27] reported buoyancy effects on turbulent velocity even at low Gr/Re^2 ratios in a vertical annular channel. Kobus and Wedekind [28] developed their models for both assisted and opposed flows from a vertical flat plate. Their numerical predictions agreed well with their experimental measurements. Parlatan et al. [29] studied the combined effects of buoyancy and varying physical properties in turbulent mixed convection. Friction factors and heat transfer coefficients were experimentally measured for turbulent water flow in a heated circular tube.

Recently, results in rotating channels [30, 31] simulating the conditions in a turbine rotor blade coolant passage reveal that mixed convection plays an important role even at significantly high Reynolds numbers, greater than 10 000, in a centrifugal body force field. Most published literatures in mixed convection were based on the test geometry with all sides heated, whereas this work is an assisted mixed convection in a vertical square channel under four different asymmetric heating conditions, i.e., with one or two sides heated. The two heated sides simulate a possible thermal loading condition [30] of a turbine rotor blade internal coolant passage with heat conducted from two opposite sides (leading and trailing sides). Heat transfer augmentation techniques used in a rotor blade coolant passage can create significant non-uniformity on the temperature distribution. These asymmetric heating models show interesting results that are reported for the first time. This paper covers the laminar, the transition, and the fully turbulent flow regimes ($200 \leqslant Re \leqslant 11\,200$) and these Reynolds numbers are ideal for direct numerical simulations (DNS). Bulk flow characteristics are reflected in the heat transfer coefficient distributions. Previous work of Dutta et al. [32] on this setup used uniform heating on both sides of the channel. An asymmetric heating, as presented here, creates a stronger three-dimensional flow disturbance that can change heat transfer characteristics both upstream and downstream.

2. Experimental apparatus and procedures

The apparatus used for the present study is identical to that of [32], as shown in Fig. 1, except that different heating conditions (as discussed later) are applied. A centrifugal pump is used to ensure the flow circulation from a large storage water tank. The flow control is achieved by a feed back flow loop from the pump to the tank bypassing the test facility. Volume flow rate is measured by calibrating water volume in a graduated container and measuring time with a stopwatch. The flow direction in the test section can be either upward or downward by selectively opening and closing valves in the flow path.

The heated test section is placed between two identical unheated channels that eliminate the inlet and exit condition irregularities created by a change in cross-section from a circular smaller diameter pipe to a larger square channel. All three sections have the same square cross-section (5.715 cm × 5.715 cm) and are 122 cm long with the same hydraulic diameter, D, 5.715 cm.

The test section is heated on two sides and the other two unheated sides are clear insulated viewing windows. There are ten heated copper plates on each heated side. Each plate is 10.16 cm × 5.08 cm in cross-section and is

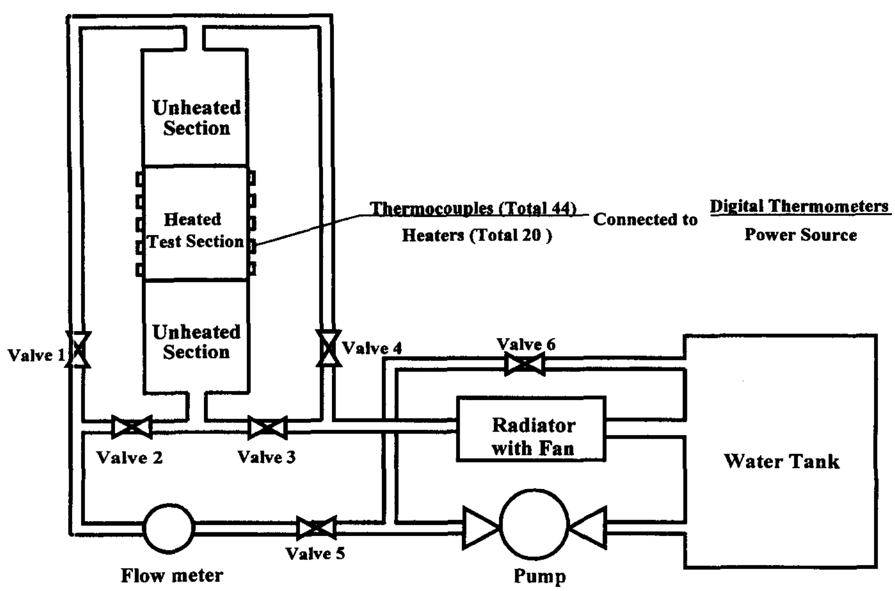

Fig. 1. Schematic setup of the test facility [32].

separated by 0.5 cm from its neighbors. Each of these plates is heated from outside by a commercial 250 watt electric strip heater. Water comes in contact with the other side of each of these heated plates and two thermocouples are used on each plate to measure the plate temperatures. An average of these two thermocouples is taken for the copper plate temperature. The inlet and exit water temperatures are measured with two thermocouples at the inlet and two at the outlet. During experimentation, inlet temperature is observed to be the same as the storage tank water temperature, thus confirming the negligible conduction effects at the upstream direction. The outlet temperature measures the core exit flow temperature and is found to be a maximum of 7% less than our calculated bulk result.

Figure 2 shows that twenty identical electric heaters are divided evenly into four groups, named groups A, B, C, and D. Each group is controlled independently by a power controller. The electrical powers to the heaters are controlled to give as close a uniform wall temperature condition as possible. Each group of heaters receives the same heat flux and thus the inter-group temperatures are controlled to be uniform. Note that the main difference between this work and the previous works [16, 18, 22, 25] is that in our case NOT all four surrounding walls are heated, instead two opposite walls are heated in four different heating conditions. In Dutta et al. [32] all group heaters, A, B, C, and D, were ON. Unlike that heating condition [32], in this experiment those four groups of heaters are selectively switched ON and OFF to get four designed heating conditions, namely models #1, #2, #3 and #4 as shown in Table 1. This asymmetric heating causes large buoyancy driven cell structures in the flow. Gau et al. [16] reported a large separated flow region due to asymmetric heating in a two-dimensional flow. For

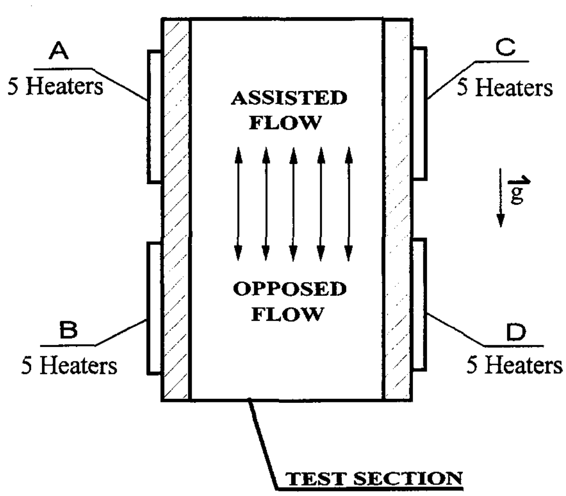

Fig. 2. Four different heater groups in the test section.

Table 1
Four heating models (see Fig. 2 for heater nomenclature)

	Group heaters Left wall		Right wall	
Model#	A	B	C	D
1	OFF	OFF	ON	OFF
2	ON	OFF	ON	OFF
3	OFF	OFF	ON	ON
4	OFF	ON	ON	OFF

this experiment the flow is three-dimensional due to the buoyancy driven secondary flow.

The local heat transfer coefficient is calculated as:

$$h = \frac{q''_{\text{total}} - q''_{\text{loss}}}{T_w - T_b} \tag{1}$$

Local bulk temperature, T_b, at any location, i, is calculated by usual heat balance technique as:

$$T_b(i) = T_b(i-1) + \frac{(q''_{\text{total}} - q''_{\text{loss}})A_{\text{plate}}}{\dot{m}c_p} \tag{2}$$

where $T_b(i)$ and $T_b(i-1)$ are consecutive bulk temperatures, and $\dot{m}$ is mass flowrate. The lost heat flux, q''_{loss}, is estimated from a different test without water flow and is less than 5% of the overall heat flux applied. The uncertainties, based on the method by Kline and McClintock [33], range from $\pm 7.6\%$ to $\pm 3.1\%$ for the Reynolds numbers and from $\pm 4.3\%$ to $\pm 2.1\%$ for the Nusselt numbers. The Reynolds number uncertainty increases and Nusselt number uncertainty decreases with an increase in the flow Re. Uncertainties in results are mostly from the resolutions of measuring devices (instrumental deviation). All physical properties of the flow, other than the thermal conductivity of water, are based on the inlet water temperature (property values are taken from Incropera and Dewitt [2]). The thermal conductivity of water, required for Nusselt number calculation, is taken at the film temperature. Film temperature is defined as the arithmetic mean of the local wall temperature and the local bulk-mean water temperature. Details of the overall flow and heating condition characteristics are listed in Table 2.

3. Results and discussions

Figures 3 and 4 show the typical wall and bulk temperature distributions for four heating models along the axial position ($0.87 \leqslant x/D \leqslant 17.1$) at highest and lowest Reynolds numbers. Each temperature profile demonstrates the heating characteristics with respect to the corresponding heating model. Average room tem-

Table 2
Actual experimental data for assisted mixed convection

Run no.	Re in figs	Actual Re	Gr	Nu_0
		Heating model #1		
1	330	329.37	1970537	8.6387
2	700	629.01	1837424	11.0643
3	1600	1591.78	2129841	14.6055
4	2500	2445.92	2356792	16.854
5	3500	3540.35	2020732	24.8409
6	4800	4789.8	2492088	34.7075
7	9600	9616.36	2280414	68.4377
		Heating model #2		
1	360	363.24	5931519	8.5802
2	800	835.33	5388679	11.3245
3	1600	1620.54	6273080	14.125
4	2700	2704.6	4253136	17.4283
5	2800	2770.4	4225528	17.5685
6	4700	4664.65	3908346	33.7511
7	9200	9208	4390612	65.784
		Heating model #3		
1	330	329.41	7148310	8.3051
2	600	624.63	5873580	10.2796
3	1100	1123.98	5547263	12.5032
4	2200	2174.48	6718315	15.5795
5	3400	3393.6	6590229	22.674
6	4500	4542.42	4309872	32.811
7	10600	10580.56	3731587	74.7361
		Heating model #4		
1	200	205.73	7114774	7.0991
2	350	345.94	6251730	8.4418
3	1100	1133.19	6288322	12.5372
4	1800	1785.96	6513995	14.5901
5	2800	2779.44	6343210	16.9078
6	4400	4374.15	6669522	30.2013
7	11200	11174.05	6230380	74.9867

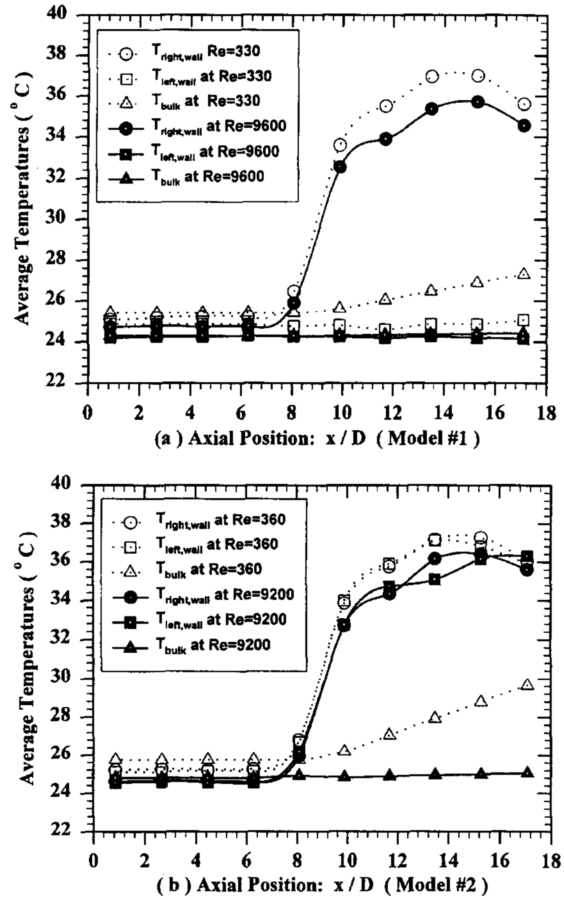

Fig. 3. Bulk and wall temperature distributions at selected Reynolds numbers for heating models #1 and #2.

perature is 21.2°C. The piece-wise linear profile of bulk temperature indicates the effect of piece-wise uniform heat flux applied. Fluctuations in the axial wall temperature distribution reflect clearly the presence of large-scale flow structures developed by the buoyancy effects.

Local Nu/Nu_0 ratio profiles as a function of axial positions (x/D) are shown in Figs 5 and 6. The actual values of the Nu_0 are listed in Table 2. Plotted data span a wide range of Reynolds numbers that varies from laminar ($Re = 200$) to fully turbulent regime ($Re = 11\,200$), and represent different Nusselt number ratio trends. In general, both Figs 5 and 6 show that the local Nusselt number ratios decrease significantly with an increase in the Reynolds number. Fluctuations in the Nu/Nu_0 ratio profile decay from laminar flow to fully turbulent flow.

Figure 5 shows similar local Nu/Nu_0 ratio profiles for both heating models #1 and #2. This fact is consistent with the similarity in their heating conditions. In the inlet region for both models #1 and #2, i.e., $9.89 < x/D < 14$, the Nu/Nu_0 ratio's decrease noticeably and then reach their minimum as the thermal boundary layer develops. After those minimum values, the effect of the buoyancy force and the development of flow reversal contributes to a gradual recovery of Nu/Nu_0 ratio as noted in the axial locations from $x/D = 14$ to the exit. This trend of recovery diminishes from the lowest Re to the highest Re. Note that the Nu/Nu_0 ratios for model #2 are higher in magnitude than those of model #1 at similar Reynolds numbers, indicating more buoyancy affected activity in model #2.

Local Nu/Nu_0 ratio profiles for models #3 and #4 are shown in Fig. 6. For model #3, a decrease in Nu/Nu_0 ratio is observed in the inlet region ($0 < x/D < 4.5$) as the thermal boundary layer develops. After reaching their lowest values, the Nu/Nu_0 ratios restore rapidly and reach their peaks due to the combined effects of buoyancy

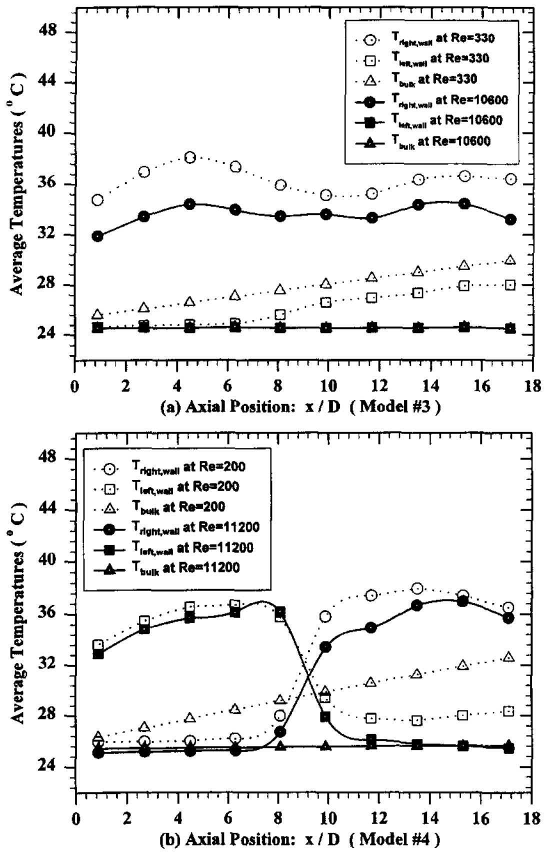

Fig. 4. Bulk and wall temperature distributions at selected Reynolds numbers for heating models #3 and #4.

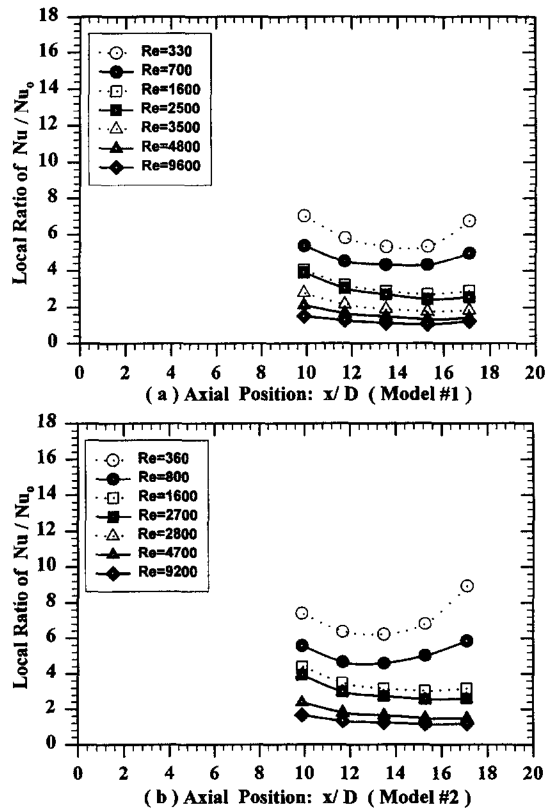

Fig. 5. Local Nusselt number ratio at different Reynolds numbers for heating conditions #1 and #2.

driven acceleration and development of flow reversal in the axial locations of $4.5 < x/D < 11.7$. In downstream regions, $11.7 < x/D < 15$, the decreasing heat transfer coefficients for laminar flow ($330 < Re < 1100$) indicate that the effect of flow reversal disappears gradually. For comparison, results from Dutta et al. [32] are also plotted and similar profiles are observed with higher Nu/Nu_0 ratios for [32]. Note that in Dutta et al. [32] all four heater-groups were ON. The observation agrees with the conclusion drawn from the comparison between models #1 and #2, i.e., more buoyancy effects are present in both sides heated condition. Model #4 shows a different pattern in Fig. 6b; Nu/Nu_0 ratio decreases through a longer region (up to x/D of 6). It means that the recovery of heat transfer coefficients is delayed due to this specific heating condition. Observed heat transfer coefficient peaks near $x/D = 9.8$ and that can be explained by the switch in the heated surfaces from left to right as the flow rises upward. In general, model #4 shows higher heat transfer coefficients than model #3 at comparable Reynolds numbers.

Overall lower Reynolds numbers show more remarkable heat transfer enhancements. A maximum of 22% increase in Nu/Nu_0 ratio is observed at $x/D = 17.1$ between models #3 and #4 under the similar heat flux and at comparable Reynolds numbers ($Re = 330$ and $Re = 350$). In contrast, as evident in the present results, not so significant difference in heat transfer coefficient (Nu/Nu_0) is observed between models #1 and #2 due to their relatively similar heating conditions. Note that the input thermal energy in model #2 is almost twice as much as that of model #1.

Figure 7 shows the variation of average Nusselt number ratio with different buoyancy-assisted levels represented by a Gr/Re ratio. The average Nusselt number is calculated as the arithmetic mean of all the local Nu's. Ramachandran et al. [9] observed an increase in laminar Nusselt numbers in assisted flow. Together with our earlier published results, the present results show significant heat transfer enhancement represented by an Nu/Nu_0 ratio with an increasing Gr/Re ratio. Present models show higher heat transfer coefficients compared with the earlier result [32] when compared at the same Gr/Re. These larger Nusselt number ratios indicate that the flow is perhaps turning turbulent due to buoyancy at low Reynolds numbers. However, the profiles with the higher level

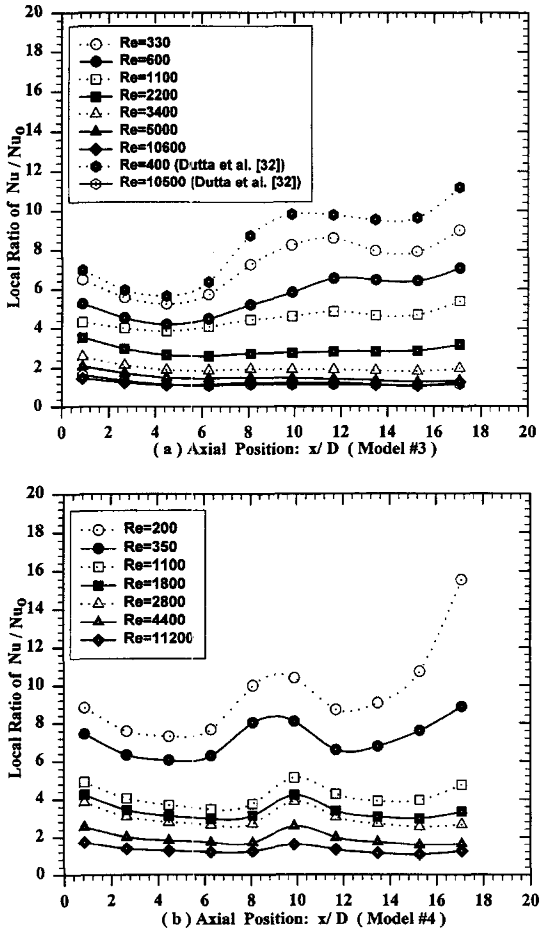

Fig. 6. Local Nusselt number ratio at different Reynolds numbers for heating conditions #3 and #4.

Nu/Nu_0 at a given Gr/Re in models #1 and #2 perhaps indicate a developing boundary layer effect. For models #1 and #2, due to limited developmental lengths (half the test section length) of buoyancy affected flow and thermal boundary layers, the buoyancy force plays a more important role in heat transfer compared to its role in models #3 and #4.

Figure 8 shows comparison between present average Nu's and previous published numerical and experimental data. Gau et al. [25] reported their results on mixed convection in a two-dimensional divergent vertical channel. The parameter $\overline{Nu}/Re^{0.4}$ is correlated in terms of Gr/Re^2 as (for assisted convection and $Gr/Re^2 \leqslant 907$):

$$100 \cdot \log(\overline{Nu}/Re^{0.4}) = -17.75 + 8.6675 \cdot \log(Gr/Re^2) + 1.5805 \cdot \log[(Gr/Re^2)]^2 \quad (3)$$

In a different study, Huang et al. [22] studied mixed convection flow in a two-dimensional vertical convergent channel and a correlation was developed for assisted convection and $Gr/Re^2 \leqslant 907$ as:

$$100 \cdot \log(\overline{Nu}/Re^{0.4}) = -3.8 + 0.4124 \cdot \log(Gr/Re^2) + 2.6234 \cdot \log[(Gr/Re^2)]^2 \quad (4)$$

Another correlation obtained from numerical calculation of natural convection in a finite vertical channel for $Gr < 10^3$ by Yan and Lin [34] can be written as:

$$\overline{Nu}/Re^{0.4} = 0.476 \cdot (Gr/Re^2)^{0.2} \quad (5)$$

Three lines in Fig. 8 indicate equations (3) to (5) for both assisted and natural convections. Our three-dimensional asymmetric heating models show much higher heat transfer levels compared to those correlations. In general, the normalized Nusselt number increases with increasing Gr/Re^2 (for $Gr/Re^2 > 1.0$) and the profile appears similar to the divergent channel profile [25]. It should be noted that the Grashof number of the present study is significantly higher than those used by Yan and Lin [34]. These asymmetrically heated results are higher than the all four-group heating condition of Ref. [32].

In Fig. 9, variations of average Nusselt number ratios with the buoyancy number are plotted. Unlike most previous published works that covered the buoyancy number, Bo, less than 10, this work spans a rather wide range of the Bo number, from 0.16 to 27 500. Our results show significantly increasing Nusselt number ratios with an increase in the Bo number. The buoyancy parameter correlation developed by Cotton and Jackson [1] for laminar assisted flow in a uniformly heated vertical tube is plotted for comparison. Presented results show a good quantitative consistency with the numerical prediction in

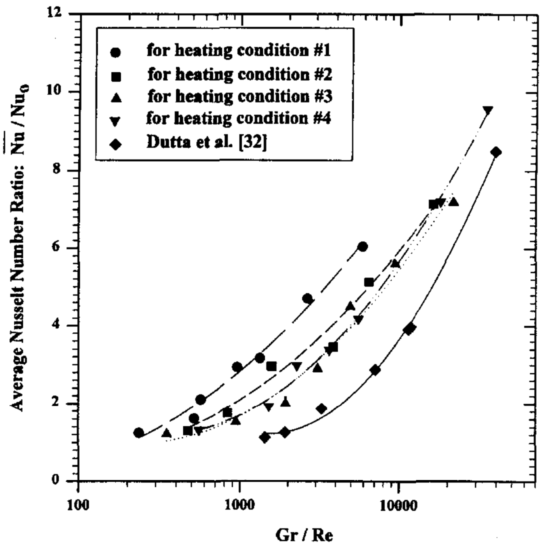

Fig. 7. Variation of average Nusselt number ratio with different assisted buoyancy levels in four different heating conditions.

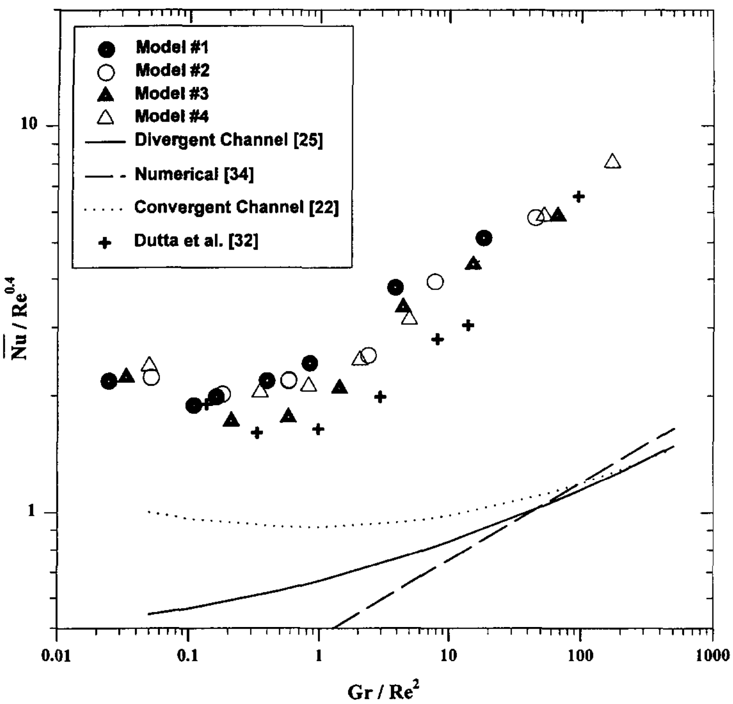

Fig. 8. Comparison of average Nusselt numbers for four heating models with previous experimental data and numerical prediction.

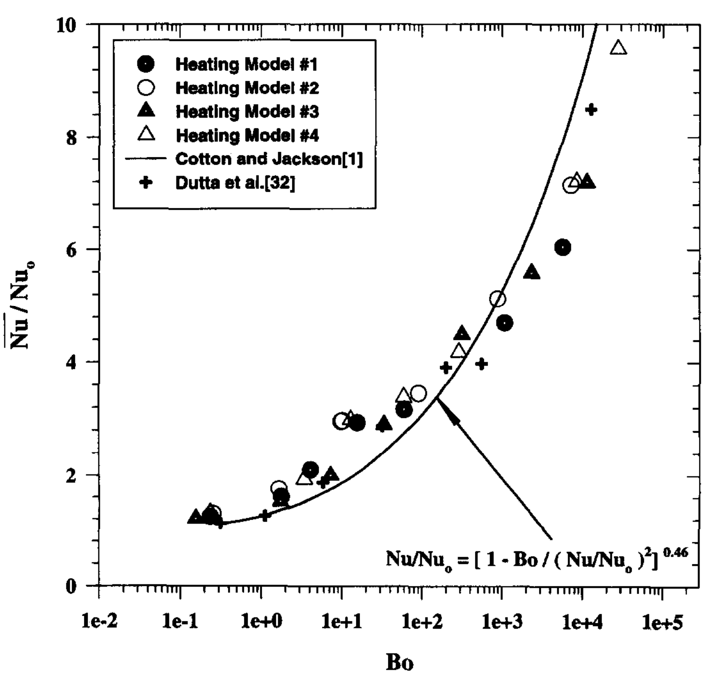

Fig. 9. Average Nusselt number ratio variations with the buoyancy number for four heating models and previous numerical prediction.

the characteristic shape, but the measured heat transfer coefficients are higher in magnitude due to axisymmetric heating. The effect of different heating conditions shows little influence in this plot. The buoyancy number includes the local heat flux and overall mass flow rate in its formulation. The local fluid temperature rise and thus the buoyancy effect is determined by the local heat flux and mass flow rate. Therefore, it can be argued that the buoyancy number can absorb the different heating condition effects more uniformly than the temperature dependent Grashof number.

4. Conclusion

Buoyancy-assisted mixed convection heat transfer in a square vertical channel under asymmetric heating conditions has been studied experimentally. The present investigation differs from most published literature on its extensive range of the Reynolds number ($200 \leqslant Re \leqslant 11\,200$), the Buoyancy number, Bo ($0.16 \leqslant Bo \leqslant 27\,500$), and asymmetric heating conditions. Four heating models (#1 to #4, see Table 1) are developed based on the combinations of four groups of heaters on two opposite sides of the square test section. The remarkable fluctuations of temperature profile reveal the presence of strong large-scale flow structures in the buoyancy-affected flow. Significant enhancement in heat transfer coefficient is noted due to the buoyancy-caused irregularities in the flow (heating conditions from model #1 to model #4) under comparable heat flux input. Heat transfer improvement from the highest Reynolds number ($Re = 11\,200$) to the lowest Reynolds number ($Re = 200$) is significant and enhancement is higher for model #4. Correlation based on the Gr/Re^2 ratio shows the present $Nu/Re^{0.4}$ ratio is more than two times higher than those of published numerical and experimental results [22, 25, 34]. Correlation based on the buoyancy parameter also gives similar results and the present data are higher compared with the previous numerical prediction [1]. The increase in heat transfer coefficient can be attributed to the three-dimensional large-scale buoyancy-induced motion in the flow field.

Acknowledgments

This project is sponsored by Research and Productive Scholarship, SPAR, USC. Contributions from project administrator Mr S. Etheredge and R & PS Committee Chair Prof. J. W. Van Zee are thankfully acknowledged.

References

[1] Cotton MA, Jackson JD. Vertical tube air flows in the turbulent mixed convection regime calculated using a low Reynolds $k-\varepsilon$ model. International Journal of Heat and Mass Transfer 1990;33:275–86.
[2] Incropera FP, DeWitt DP. Fundamentals of Heat and Mass Transfer. 4th edn. New York: John Wiley and Sons, 1996.
[3] Buhr HO, Horsten EA, Carr AD. The distortion of turbulent velocity and temperature profiles on heating for mercury in a vertical pipe. ASME Journal of Heat Transfer May, 1974;152–8.
[4] Emery AF, Dreger WW, Wyche DL, Yang A. Laminar and turbulent free convection through vertical enclosures filled with non-Newtonian fluids. ASME Journal of Heat Transfer August, 1975;366–71.
[5] Maitra D, Raju KS. Combined free and forced convection laminar heat transfer in a vertical annulus. ASME Journal of Heat Transfer February, 1975;135–7.
[6] Ou JW, Cheng KW, Lin RC. Combined free and forced laminar convection in inclined rectangular channels. International Journal of Heat and Mass Transfer 1976;19:277–83.
[7] Abdelmeguid AM, Spalding, DB. Turbulent flow and heat transfer in pipe with buoyancy effects. Journal of Fluid Mechanics 1979;94:383–400.
[8] Ljuboja M, Rodi W. Prediction of horizontal and vertical turbulent buoyant wall jets. ASME Journal of Heat Transfer 1981;103:343–9.
[9] Ramachandran N, Armaly BF, Chen TS. Measurements and predictions of laminar mixed convection flow adjacent to a vertical surface. ASME Journal of Heat Transfer 1985;107:636–41.
[10] Krishnamurthy R, Gebhart B. Heat transfer by mixed convection in a vertical flow undergoing transition. International Journal of Heat and Mass Transfer 1986;29:1211–8.
[11] Shai I, Barnea Y. Simple analysis of mixed convection with uniform heat flux. International Journal of Heat and Mass Transfer 1986;29:1139–47.
[12] Yao LS. Two-dimensional mixed convection along a flat plate. ASME Journal of Heat Transfer 1987;109:440–5.
[13] Tewari SS, Jaluria Y. Mixed convection heat transfer from thermal sources mounted on horizontal and vertical Surfaces. ASME Journal of Heat Transfer 1990;112:975–87.
[14] Lin TY, Hsieh SS. Natural convection of opposing/assisting flows in vertical channels with asymmetrically discrete heated ribs. International Journal of Heat and Mass Transfer 1990;33:2295–309.
[15] Cheng CH, Kou HS, Huang WH. Flow reversal and heat transfer of fully developed mixed convection in vertical channels. AIAA Journal of Thermophysics and Heat Transfer 1990;4:375–83.
[16] Gau C, Yih KA, Aung W. Reversed flow structure and heat transfer measurements for buoyancy-assisted convection in a heated vertical duct. ASME Journal of Heat Transfer 1992;114:928–35.
[17] Choi CY, Ortega A. Mixed convection in an inclined channel with a discrete heat source. International Journal of Heat and Mass Transfer 1993;36:3119–34.
[18] Cheng CH, Weng CJ. Developing flow of mixed convection in a vertical rectangular duct with one heating wall. Numerical Heat Transfer 1993;24:479–93.
[19] Cheng CH, Yang JJ. Buoyancy-induced recirculation bub-

bles and heat convection of developing flow in vertical channels with fin arrays. International Journal of Heat and Fluid Flow 1994;15:11–9.

[20] Fu G, Todreas NE, Hejzlar P, Dricoll MJ. Heat transfer correlation for reactor riser in mixed convection air flow. ASME Journal of Heat Transfer 1994;116:489–92.

[21] Jackson JD, Cotton MA, Axcell BP. Studies of mixed convection in vertical tubes. International Journal of Heat and Fluid Flow 1989;10:2–15.

[22] Huang TM, Gau C, Aung W. Mixed convection flow and heat transfer in a heated vertical convergent channel. International Journal of Heat and Mass Transfer 1995;38:2445–56.

[23] Joye DD. Comparison of correlations and experiment in opposing flow, mixed convection heat transfer in a vertical tube with Grashof number variation. International Journal of Heat and Mass Transfer 1996;39:1033–8.

[24] Ligrani PM, Choi S. Mixed convection in straight and curved channels with buoyancy orthogonal to the forced flow. International Journal of Heat and Mass Transfer 1996;39:2473–84.

[25] Gau C, Huang TM, Aung W. Flow and mixed convection heat transfer in a divergent heated vertical channel. ASME Journal of Heat Transfer 1996;118:606–14.

[26] Wang L, Cheng KC. Flow transition and combined free and forced convection heat transfer in a rotating curved circular tube. International Journal of Heat and Mass Transfer 1996;39:3381–400.

[27] Velidandla V, Putta S, Roy RP. Turbulent velocity field in isothermal and heated liquid flow through a vertical annular channel. International Journal of Heat and Mass Transfer 1996;39:3333–46.

[28] Kobus CJ, Wedekind GL. Modeling the local and average heat transfer coefficient for an isothermal vertical flat plate with assisting and opposing combined forced and natural convection. International Journal of Heat and Mass Transfer 1996;39:2723–33.

[29] Parlatan Y, Todreas NE, Driscoll MJ. Buoyancy and property variation effects in turbulent mixed convection of water in vertical tubes. ASME Journal of Heat Transfer 1996;118:381–7.

[30] Han JC, Zhang YM, Kalkuehler K. Uneven wall temperature effect on local heat transfer in a rotating two-pass square channel with smooth walls. ASME Journal of Heat Transfer 1993;115:912–20.

[31] Wagner JH, Johnson BV, Kopper FC. Heat transfer in rotating serpentine passage with smooth walls. ASME Journal of Turbomachinery 1991;113:321–30.

[32] Dutta S, Zhang XD, Khan J, Bell D. Heat transfer analysis in a two-sided heated smooth square vertical channel with adverse and favorable mixed convection. National Heat Transfer Conference. Maryland, Baltimore. HTD—Vol. 346, 10–2 August 1997;8:119–25.

[33] Kline SJ, McClintock FA. Describing uncertainties in single-sample experiments. Mechanical Engineering 1953;3–8.

[34] Yan WM, Lin TF. Natural convection heat transfer in vertical open channel flows with discrete heating. Proceedings of 3rd National Conference on Mechanical Engineering, CSME 1986;157–67.